OPEN ACCESS
The Journal of Engineering and Exact Sciences – jCEC, Vol. 08 N. 03 (2022)
journal homepage: https://periodicos.ufv.br/jcec
eISSN: 2527-1075
ISSN: 2446-9416

Electronic Angular Tunneling Effect

Efeito do Tunelamento Angular Eletrônico

Article Info:
Article history: Received 2022-05-04 / Accepted 2022-05-26 / Available online 2022-05-26
doi: 10.18540/jcecvl8iss3pp14294-01e

Jorge Henrique Sales
ORCID: https://orcid.org/0000-0003-1992-3748
Universidade Estadual de Santa Cruz, Brasil
E-mail: jhosales@uesc.br
Cássio Almeida Lima
ORCID: https://orcid.org/0000-0003-0841-135X
Instituto Federal da Bahia, Brasil
E-mail: cassiolima@ifba.edu.br
Gislan Silveira Santos
ORCID: https://orcid.org/0000-0002-9067-5815
Instituto Federal da Bahia, Brasil
E-mail: gislan.santos@ifba.edu.br
Alfredo Takashi Suzuki
ORCID: https://orcid.org/0000-0002-5995-0276
La Sierra University, Physics Department, Riverside, CA 92505, United States
E-mail: asuzuki@lasierra.edu

Abstract
In this article we show that the probability for an electron tunneling a rectangular potential barrier depends on its angle of incidence measured with respect to the normal line. The majority of the studies in the field consider a one-dimensional tunneling of an electron of mass m in a potential barrier along the x-axis. Using a two-dimensional approach, we observed that the angle of incidence of the electron influences the probability of tunneling.
Keywords: Potential barrier. Angular Tunneling. Two-dimensional.

Resumo
Neste trabalho mostramos que a probabilidade de um elétron tunelar em uma barreira de potencial retangular depende do seu ângulo de incidência medido em relação à linha normal. A maioria dos estudos na área considera um tunelamento unidimensional de um elétron de massa m em uma barreira de potencial ao longo do eixo x. Usando uma abordagem bidimensional, observamos que o ângulo de incidência do elétron influencia na probabilidade de tunelamento.
Palavras-chave: Barreira de potencial. Tunelamento Angular. Bidimensional.

1. Introduction

According to the principles of classical physics, a particle of energy E which is smaller than the height V of a potential barrier can not penetrate it – the region inside the barrier is classically forbidden. Quantum mechanics, however, allows for the so-called tunneling effect, in which due to the fact that the wave function associated with a free particle must be continuous at the barrier it will show an exponential decay inside the barrier (SAKURAI, 1994), thus accounting for a non-zero probability of finding the particle inside the barrier.

In most of the one-dimensional problems we study the motion of a particle approaching the barrier occurs from the left with an angle $\theta = 0^0$ (i.e., normal to the barrier) and then penetrating the barrier. Depending on whether $E > V$ or $E < V$ the particle can pass through the potential or be reflected back.

In two or three dimensions when the barrier is only a function of the distance from the origin of the coordinate system, i.e. $\rho = \sqrt{x^2 + y^2}$ or $r = \sqrt{x^2 + y^2 + z^2}$, we can separate the variables in the Schrödinger equation and thus reduce the problem to a one-dimensional motion but now with the boundary conditions imposed at $\rho = 0$ or $r = 0$ and at ρ and r going to infinity (BENDERSKII, 1991; BOWCOCK, 1991; BRACHER, 1998). For instance, in three dimensions if we assume that $V(r \longrightarrow \infty) \longrightarrow 0$ and that $V(r)$ has a maximum at $r = L$, then if the particle is originally confined within the region $0 < r < L$, it can tunnel through the barrier and go to infinity (HUANG, 1990; RING, 1977; SCHMID, 1986).

The interest in such studies are real experimental realizations, e.g., in 2000 the tunneling effect was studied as an application in nuclear deformation on the alpha-decay (DIMARCO, 2000). A more general study, Fredholm Method, is presented in the works of Sales (SALES et al, 2021; SALES; GIROTTO, 2021)

Since the wave function must also be continuous on the far side of the barrier, there is a non-zero finite probability that the particle will tunnel through the barrier. Such experimental scenario suggests we define the rectangular potential barrier as:

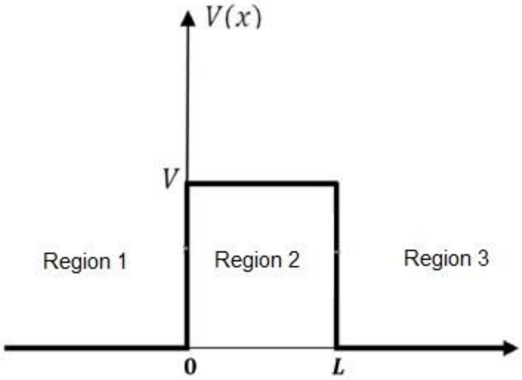

Figure 1 – One-dimensional square potential.

$$\begin{cases} \quad = 0, for\ x < 0 \longrightarrow Region\ 1 \\ V > 0, for\ 0 \leq x \leq L \longrightarrow Region\ 2 \\ \quad = 0, for\ x > L \longrightarrow Region\ 3. \end{cases}$$

We define the transmission coefficient T as the measure of the probability for a particle coming from the left hand side, *Region 1*, incident on the barrier, *Region 2*, to be tunneling through it and continuing to travel to the right hand side of it, *Region 3* (see Figure 1). It can be evaluated by:

$$T = 16\frac{E}{V}\left(1 - \frac{E}{V}\right)e^{-2kl}, \tag{1}$$

where

$$k = \frac{1}{\hbar}\sqrt{2m(V - E)}. \tag{2}$$

Equation (1) shows us that a particle with mass m and energy $E < V$, that approaches a potential barrier with height V and width L has a probability $T \neq 0$ of penetrating the barrier and even appearing on the other side. This phenomenon is known as tunneling (TAKADA, 1994; WANG, 1986; ZAMASTIL, 2001).

2. Transmission Through a Potential Barrier

The model we present in this section serves for scattering, collimated and nearly mono-energetic beam of particles. We also make the assumption that eventual dispersions of the wave that may occur will be disregarded. So, if a free particle of mass m and energy E approaches the barrier from *Region 1* with an angle of incidence $\theta \neq 0$ with respect to the normal line of the potential barrier with height V and width L, the eigenfunctions are obtained from the solution of the Schrödinger equation and are:

$$\psi(\vec{r}) = \begin{cases} Ae^{i\vec{k}_1\cdot\vec{r}} + Be^{-i\vec{k}_1\cdot\vec{r}}\ (r < 0) \\ Ce^{i\vec{k}_2\cdot\vec{r}} + De^{-i\vec{k}_2\cdot\vec{r}}\ (0 < r < L), \\ Fe^{i\vec{k}_3\cdot\vec{r}}\ (r > L) \end{cases} \tag{3}$$

where $\vec{r}$ is the position vector, and $\vec{k}_1$, $\vec{k}_2$ and $\vec{k}_3$ are the wave numbers $\left(\vec{k}_1 = \vec{p}_1/\hbar\right)$ for each region, with $\vec{p_i}$ the particle momentum, and $i = 1, 2, 3$. We now explicit the scalar products that appear in the exponentials as

$$\vec{k}_1 \cdot \vec{r} = k_1 r \cos\theta, \tag{4}$$

$$\vec{k}_2 \cdot \vec{r} = k_2 r \cos\theta_{ref}, \tag{5}$$

$$\vec{k}_3 \cdot \vec{r} = k_3 r \cos\theta_3. \tag{6}$$

With no loss of generality, we may assume that the absolute refractive index for *Region 1* is the same as the one for *Region 3*, i.e., $n_1 = n_3$. By Snell's refraction law this implies that $\theta_3 = \theta$, and therefore, $k_3 = k_1$.

Using now the expression for the probability current density

$$\vec{J} = \frac{i\hbar}{2m}\left(\Psi\vec{\nabla}\Psi^* - \Psi^*\vec{\nabla}\Psi\right), \tag{7}$$

we obtain the three probability current densities for the corresponding eigenfunctions

$$\vec{J}_{inc} = \frac{k_1\hbar}{m}|A|^2\left(\cos\theta\,\hat{\boldsymbol{r}} - \frac{\sin\theta}{r}\hat{\theta}\right), \tag{8}$$

$$\vec{J}_{refl} = -\frac{k_1\hbar}{m}|B|^2\left(\cos\theta\,\hat{\boldsymbol{r}} - \frac{\sin\theta}{r}\hat{\theta}\right), \tag{9}$$

$$\vec{J}_{trans} = \frac{k_1\hbar}{m}|F|^2\left(\cos\theta\,\hat{\boldsymbol{r}} - \frac{\sin\theta}{r}\hat{\theta}\right). \tag{10}$$

Here $\vec{J}_{inc}$ is the incident current density for the incoming wave in *Region 1*, $\vec{J}_{refl}$ the reflected current density for the reflected wave to *Region 1*, while$\vec{J}_{trans}$ is the transmitted current density to *Region 3*. So,

$$R_{angular} = \frac{|\vec{J}_{refl}|}{|\vec{J}_{inc}|} = \left|\frac{B}{A}\right|^2 \tag{11}$$

is the *reflection coefficient*, defined as the probability that an particle is reflected at the barrier. Similarly,

$$T_{angular} = \frac{|\vec{J}_{trans}|}{|\vec{J}_{inc}|} = \left|\frac{F}{A}\right|^2 \tag{12}$$

is the *transmission coefficient*, defined as the probability that the particle will be transmitted to *Region 3* and A, B, F are amplitudes of *incident*, *reflected* and *transmitted* waves, respectively. The quantity $T_{angular}$ must be interpreted as the ratio of the transmitted to the incident probability current density for $E > V$.

2.1 Application of Boundary Conditions

The boundary conditions for the continuity of the wave function across the edges of the potential barrier (i.e. $r = 0$ and $r = L$) allow the coefficients in the general solutions (A, B, C, D, and F) to be found. The boundary conditions at $r = 0$ and $r = L$ are as follows:

$$\psi_1(0) = \psi_2(0), \qquad \left.\frac{\partial\psi_1}{\partial r}\right|_{r=0} = \left.\frac{\partial\psi_2}{\partial r}\right|_{r=0}, \tag{13}$$

$$\psi_2(L) = \psi_3(L), \qquad \left.\frac{\partial\psi_2}{\partial r}\right|_{r=L} = \left.\frac{\partial\psi_3}{\partial r}\right|_{r=L}. \tag{14}$$

Evaluating the partial derivatives, we have

$$\frac{\partial\psi_1}{\partial r} = ik_1 r\cos\theta\left(Ae^{i\vec{k}_1\cdot\vec{r}} + Be^{-i\vec{k}_1\cdot\vec{r}}\right), \tag{15}$$

$$\frac{\partial\psi_2}{\partial r} = ik_2 r\cos\theta_{refl}\left(Ce^{i\vec{k}_2\cdot\vec{r}} - De^{-i\vec{k}_2\cdot\vec{r}}\right), \tag{16}$$

$$\frac{\partial\psi_3}{\partial r} = ik_1 r\cos\theta\left(Fe^{i\vec{k}_1\cdot\vec{r}}\right). \tag{17}$$

For the convenience of later manipulations we introduce the following definitions

$$Z_1 = e^{ik_1 L\cos\theta},$$

$$Z = e^{ik_2 L\cos\theta_{refl}}. \tag{18}$$

Then, from the boundary conditions at $r = 0$ we obtain,

$$\psi_1(0) = \psi_2(0) \longrightarrow A + B = C + D \tag{19}$$

and from continuity in relation (13) at point $r = 0$ we get

$$\frac{\partial\psi_1(0)}{\partial r} = \frac{\partial\psi_2(0)}{\partial r} \longrightarrow ik_1\cos\theta\,(A - B) = ik_2\cos\theta_{refl}\,(C - D),$$

from which we may express A and B coefficients in terms of C and D as follows:

$$A - B = n\frac{\cos\theta_{refl}}{\cos\theta}(C - D), \tag{20}$$

where we introduced the notation $n = \frac{k_2}{k_1}$.

In a similar manner, applying the boundary condition at $r = L$, we get

$$\psi_2(L) = \psi_3(L) \longrightarrow Ce^{ik_2 L\cos\theta_{refl}} + De^{-ik_2 L\cos\theta_2} = Fe^{ik_1 L\cos\theta},$$

from which, using Eq. (18) we have

$$ZC + \frac{1}{Z}D = Z_1 F. \tag{21}$$

The continuity relation for the derivatives at $r = L$ gives us the remaining relation among the coefficients:

$$\frac{\partial\psi_2(L)}{\partial r} = \frac{\partial\psi_3(L)}{\partial r} \longrightarrow$$

$$CZ - \frac{1}{Z}D = \frac{Z_1}{n}\frac{\cos\theta}{\cos\theta_{refl}}F. \tag{22}$$

Summing up Eqs. (21) and (22), we may solve for C and D respectively obtaining:

$$C = \frac{Z_1}{2Z}\left(1 + \frac{\cos\theta}{\cos\theta_{refl}}\right)F \tag{23}$$

and

$$D = \frac{Z_1 Z}{2}\left(1 - \frac{\cos\theta}{n\cos\theta_{refl}}\right)F. \tag{24}$$

Since we want to express A in terms of F, next we solve the following system of linear equations from Eqs. (19) and (20):

$$A + B = (C + D)$$

$$A - B = n\alpha^{-1}(C - D), \tag{25}$$

were $\alpha = \frac{\cos\theta}{\cos\theta_{refl}}$.

Solving the system Eq. (25) in terms of A results in the following:

$$A = \frac{1}{2}[(1 + n\alpha^{-1})C - (n\alpha^{-1} - 1)D]. \tag{26}$$

Now introducing the results Eqs. (23) and (24) we may express the coefficient A in term of the coefficient F as

$$A = \frac{1}{4}\frac{Z_1\alpha}{NZ}(N + 1)^2\left[1 - \left(\frac{N-1}{N+1}\right)^2 Z^2\right]F, \tag{27}$$

where we have used the notation

$$N = n\alpha^{-1}. \tag{28}$$

Thus, finally Eq. (12) can be rewritten as

$$T_{angular} = \left| \frac{4NZ}{Z_1(N+1)^2\left[1-\left(\frac{N-1}{N+1}\right)^2 Z^2\right]} \right|^2. \tag{29}$$

Equation (29) is the angular transmission probability of a particle across a potential barrier with $E > V$.

3. Angular Tunneling Effect

In the case of tunneling ($0 < E < V$), the eigenfunction for *Region 2* is

$$\psi_2(r) = Ce^{\vec{k}\cdot\vec{r}} + De^{-\vec{k}\cdot\vec{r}}, \qquad (0 \le r \le L)$$

where k_2 is now defined as

$$k_2 = i|k_2| = \frac{i}{\hbar}\sqrt{2m(V-E)} \equiv ik, \qquad k > 0,$$

and

$$k = \frac{1}{\hbar}\sqrt{2m(V-E)}.$$

Here, however, we cannot exclude the exponentially increasing part of the exponential because r does not extend to $-\infty$ (boundary region) because we have a limit to the potential that is up to $r = L$. Another important fact is that the index of refraction becomes imaginary, i.e.

$$n = \frac{k_2}{k_1} = i\,\frac{k}{k_1} = i\eta, \qquad (\eta > 0).$$

Thus N as given in Eq. (28) now becomes

$$N = i\sqrt{\frac{\eta^2+(\sin\theta)^2}{1-(\sin\theta)^2}} \equiv i\beta,$$

with

$$\beta = \sqrt{\frac{\eta^2+(\sin\theta)^2}{1-(\sin\theta)^2}}.$$

Substituting N into Eq. (29), we obtain

$$T_{angular} = \left| \left[\frac{\frac{4i\beta}{(i\beta+1)^2}}{1-\left(\frac{i\beta-1}{i\beta+1}\right)^2 e^{-2kL}} \right] e^{-kL-ik_1L} \right|^2. \tag{30}$$

Here we introduce our first approximation considering the case of a thick barrier in which $kL \gg 1$. In this case we may neglect the term proportional to e^{-2kL} in the denominator of Eq. (30), yieldding

$$T_{angular} = \frac{16\beta^2}{(\beta^2+1)^2} e^{-2kL}. \tag{31}$$

Next, we express the quantities η and β in terms of the experimental values of the particle energy E and potential barrier's height V, so that after some algebraic manipulations we get for η and β

$$\eta = \frac{k}{k_1} = \frac{\frac{i}{\hbar}\sqrt{2m(V-E)}}{\frac{i}{\hbar}\sqrt{2mE}} = \sqrt{\frac{V-E}{E}} \qquad \text{or}$$

$$\eta^2 = \frac{V-E}{E}, \qquad \text{and} \tag{32}$$

$$\beta^2 = \frac{V}{E(\cos\theta)^2} - 1, \qquad \text{or}$$

$$\beta^2 + 1 = \frac{V}{E(\cos\theta)^2}. \tag{33}$$

Thus, finally we may express the angular tunneling probability Eq. (31) as

$$T_{angular} = 16\frac{E_\theta}{V}\left(1 - \frac{E_\theta}{V}\right) e^{-2k_\theta L}, \tag{34}$$

where

$$E_\theta = E(\cos\theta)^2,$$

$$k_\theta = \frac{1}{\hbar}\sqrt{2m(V - E_\theta)}.$$

Equation (34) gives us the tunneling probability of an particle that strikes in a potential barrier with an angle $\theta \neq 0$ with respect to the normal line to the barrier. We cannot fail to see the similarity between Eq. (34) and Eq. (1), and in the limit of $\theta \longrightarrow 0$ of Eq. (34) we get exactly Eq. (1).

4. Numerical Results

For the sake of clarifying the analytical/theoretical results, we did the following numerical calculations. Let us assume a rectangular barrier of height 12 eV and width 0.18 nm. From Eq. (34) we calculate the tunneling probability of finding a electron hitting in a potential barrier with angles between $-\frac{\pi}{2}$ and $\frac{\pi}{2}$, and kinetic energy varying from 0 to 12 eV (see Figure 2). The first conclusion we have drawn is that the angular tunneling probability is not zero when the electron energy E is equal to the potential barrier V. Even for small angles, there are non-vanishing angular probabilities for $E = V$.

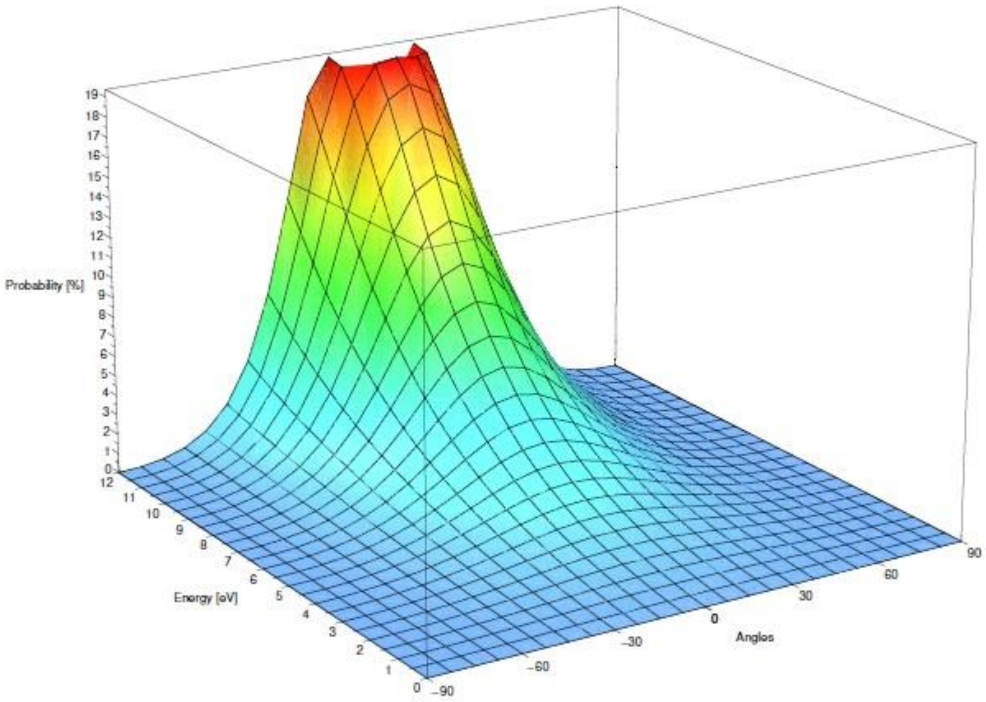

Figure 2 - Electron angular tunnelling through a barrier.

In Figures 3 and 4 we compare the one-dimensional tunneling with the angular tunneling for angles between 14° and 19°. We can clearly see that while the probability curve of the one-dimension tunneling tends to zero as the electron energy approaches the energy of the potential barrier, the probability curve of angular tunneling remains above 18% for the range of angles above mentioned when $E = V$.

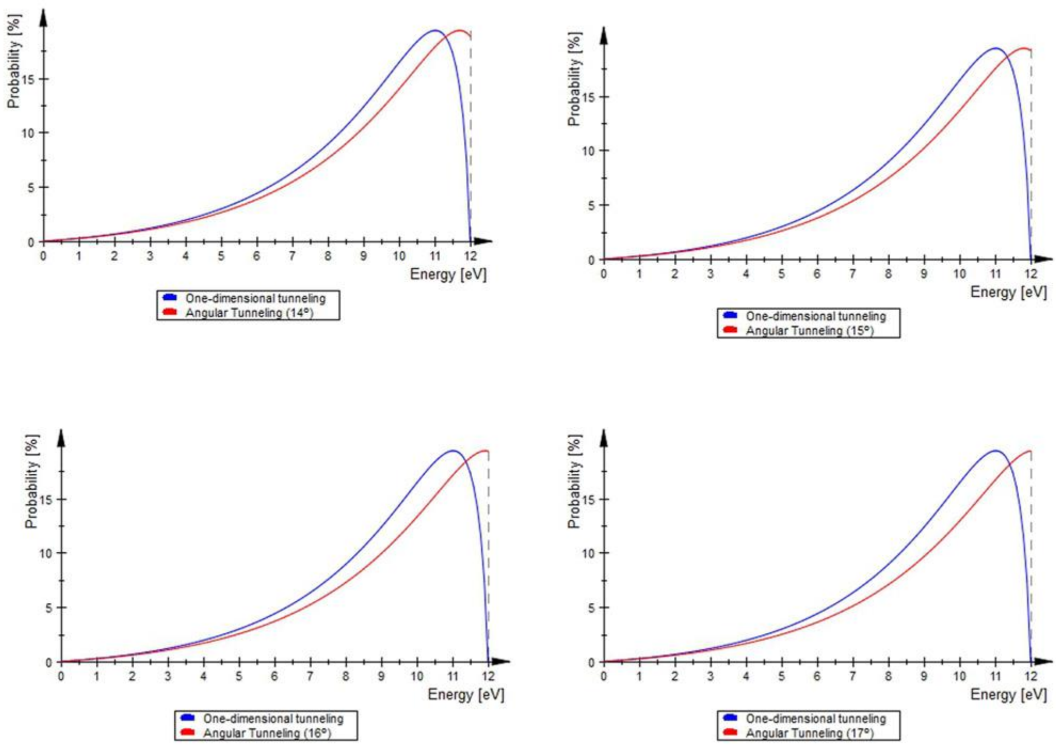

Figure 3 – Angular tunneling for $\boldsymbol{\theta = (14^{\circ}, 15^{\circ}, 16^{\circ}, 17^{\circ})}$.

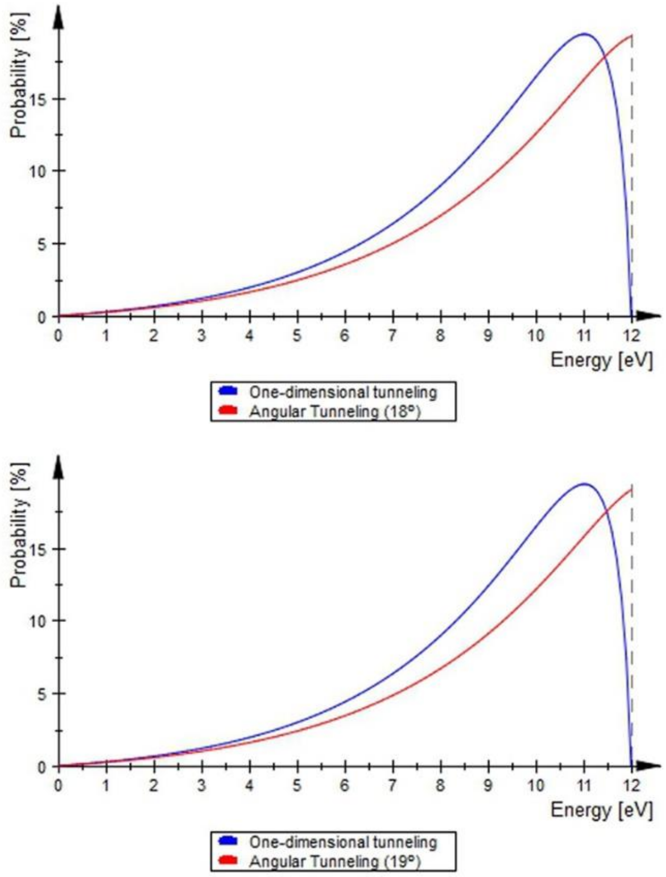

Figure 4 – Angular tunneling for $\theta = 18^\circ$ and $\theta = 19^\circ$.

Here we are interested in calculating the maximum points of the Eq. (34) using the Hessian determinant, which is defined by

$$H(E,\theta) = \begin{vmatrix} \frac{\partial^2 T_{angular}}{\partial E^2} & \frac{\partial^2 T_{angular}}{\partial \theta \partial E} \\ \frac{\partial^2 T_{angular}}{\partial E \partial \theta} & \frac{\partial^2 T_{angular}}{\partial \theta^2} \end{vmatrix} \tag{35}$$

In order to determinate the critical points, the following conditions must be satisfied, namely:

$$H(E,\theta) > 0,$$

$$\frac{\partial^2 T_{angular}}{\partial E^2} < 0,$$

$$\frac{\partial^2 T_{angular}}{\partial \theta^2} < 0. \tag{36}$$

First of all we need to solve the following system of linear equations:

$$\begin{cases} \frac{\partial T_{angular}}{\partial E} = 0, \\ \frac{\partial T_{angular}}{\partial \theta} = 0. \end{cases} \tag{37}$$

These can be evaluated through expliciting the partial derivatives:

$$\begin{cases} -\frac{4\sigma_1 \cos(\theta)^2 \varepsilon(\theta)}{3} - \frac{E\sigma_1 \cos(\theta)^4}{9} - \frac{6.63\times10^{-25} E\sigma_1 \cos(\theta)^4 \varepsilon(\theta)}{\sigma_2} = 0 \\ \frac{2E^2\sigma_1 \cos(\theta)^3 \sin(\theta)}{9} + \frac{8E\sigma_1 \cos(\theta) \sin(\theta) \varepsilon(\theta)}{3} + \frac{1.33\times10^{-24} E^2 \cos(\theta)^3 \sin(\theta) \varepsilon(\theta)}{\sigma_2} = 0 \end{cases} \tag{38}$$

where for convenience we have defined

$$\varepsilon(\theta) = \left(\frac{E \cos(\theta)^2}{12} - 1\right), \tag{39}$$

$$\sigma_1 = e^{-3.41\times10^{24}} \sigma_2, \tag{40}$$

$$\sigma_2 = \sqrt{3.49 \times 10^{-48} - 2.91 \times 10^{-49} E \cos(\theta)^2}. \tag{41}$$

Hence the system Eq. (38) is comprised of transcendental equations that we couldn't solve by using analytical methods in order to find the maximum points. With the aid of Table 1 and Figure 5 (using Eq. (35)), we have seen that the maximum points are between 0° and 25°, and energy of 10 eV to 12 eV. In Figure 5 we see a discontinuous ("white") region, showing that the Hessian is more negative towards the other, i.e, a region is "strongly" of saddle points in relation to the other.

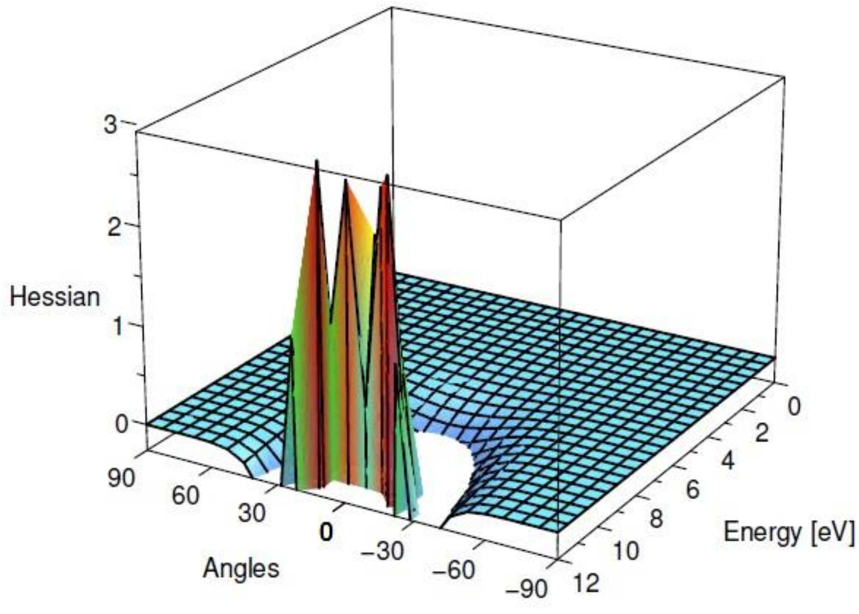

Figure 5 – Hessian.

Table 1 – Numerical table ($\times 10^{-9}$).

	10 eV				11 eV				12 eV			
Angles	**Hessian**	$\frac{\partial^2 T_{angular}}{\partial E^2}$	$\frac{\partial^2 T_{angular}}{\partial \theta^2}$	%	**Hessian**	$\frac{\partial^2 T_{angular}}{\partial E^2}$	$\frac{\partial^2 T_{angular}}{\partial \theta^2}$	%	**Hessian**	$\frac{\partial^2 T_{angular}}{\partial E^2}$	$\frac{\partial^2 T_{angular}}{\partial \theta^2}$	%
0°	0.0046	−0.0055	−0.8252	16.42	0.0054	−0.1060	−0.0514	19.37	–	–	–	–
1°	0.0045	−0.0054	−0.8257	16.40	0.0062	−0.1051	−0.0746	19.36	–	–	–	–
2°	0.0043	−0.0052	−0.8270	16.37	0.0084	−0.1024	−0.1423	19.36	–	–	–	–
3°	0.0039	−0.0047	−0.8287	16.30	0.0117	−0.0980	−0.2487	19.35	–	–	–	–
4°	0.0034	−0.0041	−0.8300	16.21	0.0157	−0.0922	−0.3850	19.34	–	–	–	–
5°	0.0028	−0.0034	−0.8298	16.10	0.0197	−0.0853	−0.5403	19.31	–	–	–	–
6°	0.0021	−0.0025	−0.8271	15.96	0.0233	−0.0776	−0.7031	19.27	–	–	–	–
7°	0.0013	−0.0016	−0.8208	15.80	0.0261	−0.0695	−0.8620	19.20	–	–	–	–
8°	0.0004	−0.0007	−0.8099	15.61	0.0279	−0.0611	−1.0068	19.11	–	–	–	–
9°	–	–	–	–	0.0284	−0.0528	−1.1292	18.99	–	–	–	–
10°	–	–	–	–	0.0277	−0.0448	−1.2234	18.83	–	–	–	–
11°	–	–	–	–	0.0259	−0.0373	−1.2857	18.64	–	–	–	–
12°	–	–	–	–	0.0233	−0.0304	−1.3148	18.41	–	–	–	–

13°	–	–	–	–	0.0201	−0.0242	−1.3113	18.13	–	–	–	–
14°	–	–	–	–	0.0166	−0.0187	−1.2774	17.82	–	–	–	–
15°	–	–	–	–	0.0129	−0.0138	−1.2164	17.47	–	–	–	–
16°	–	–	–	–	0.0094	−0.0097	−1.1322	17.08	–	–	–	–
17°	–	–	–	–	0.0061	−0.0063	−1.0294	16.66	0.0114	−0.0835	−4.5900	19.36
18°	–	–	–	–	0.0031	−0.0034	−0.9126	16.21	0.0267	−0.0612	−4.0176	19.23
19°	–	–	–	–	0.0005	−0.0011	−0.7860	15.73	0.0299	−0.0442	−3.4586	18.98
20°	–	–	–	–	–	–	–	–	0.0270	−0.0312	−2.9239	18.63
21°	–	–	–	–	–	–	–	–	0.0215	−0.0213	−2.4211	18.19
22°	–	–	–	–	–	–	–	–	0.0154	−0.0139	−1.9554	17.67
23°	–	–	–	–	–	–	–	–	0.0095	−0.0083	−1.5296	17.10
24°	–	–	–	–	–	–	–	–	0.0046	−0.0042	−1.1451	16.48
25°	–	–	–	–	–	–	–	–	0.0006	−0.0012	−0.8016	15.82

Table 1 shows maximum points between angle and energy, and its probabilities, respectively. What draws our attention is that for $\theta = 0^\circ$ there is no maximum point when electron energy is equal to the potential barrier energy, differently to what happens for angles between 17° and 25°. Even though we couldn't solve the system of transcendental functions (Eq. (38)) using analytical methods in order to find the maximum points, Table 1 was essential because it lists where the hessian is positive and the second derivatives for E and θ are both negative, which point out the maximum points (between 0° and 25°).

5. Conclusions

In this paper we have developed quantum tunneling of a particle of mass m depending on its angle of incidence with the normal line to the surface of the potential barrier. The results showed that the angular tunneling, for the case of electron striking in a potential barrier of 12 eV and a thickness of 0.18 nm, is more favorable than the usual tunneling ($\theta = 0^\circ$) for angles between 0° and 25° and energy from 10 eV to 12 eV. It was noted that the probability of angular tunneling is not equal to zero when the electron energy E is equal to the potential barrier V, unlike the usual tunneling. Even for small angles, there are angular tunneling probability when $E = V$.

Acknowledgements

JHS thanks IFT for hospitality and FAPESB Propp-00220.1300.1088 for financial support; CL thanks IFBA; GSS thanks IFBA.

References

Benderskii, V. A., Goldanskii, V. I., & Makarov, D. E. (1991). Two-dimensional tunneling in a potential with two transition states. *Chemical Physics Letters*, (186), 517-521. doi: https://doi.org/10.1016/0009-2614(91)90461-H

Bowcock, P., & Gregory, R. (1991). Multidimensional tunneling and complex momentum. *Phys. Rev. D*, (44), 1774-1785. doi: https://doi.org/10.1103/PhysRevD.44.1774

Bracher, C., Becker, W., Gurvitz, S. A., Kleber, M., & Marinov, M. S. (1998). Three-dimensional tunneling in quantum ballistic motion. *American Journal of Physics*, (66), 38. doi: https://doi.org/10.1119/1.18806

Dimarco, A. J, et al. (2000). Effect of nuclear deformation on the alpha-decay half-life of even-even alpha emitters. *International Journal of Modern Physics E*, (09), 205-219. doi: https://doi.org/10.1142/S0218301300000143

Huang, Z. H., Feuchtwang, T. E., Cutler, P. H., & Kazes, E. (1990). Wentzel-Kramers-Brillouin method in multidimensional tunneling. *Phys. Rev. D*, (41), 32-41. doi: https://doi.org/10.1103/PhysRevA.41.32

Ring, P., Rasmussen, J. O., & Massmann, H. (1977). Barrier penetration theory in more than one dimension. *Sov. J. Particles Nucl*, (7), 366. doi: https://www.osti.gov/biblio/7256302

Sakurai, J. J. (1994). *Modern Quantum Mechanics*. Revised Edition, Addison-Wesley Publishing Company.

Sales, J.H.O., Girotto, P. & Soglia, L. V. (2021). Computational Model of the Fredholm Method Applied to Podolsky Quantum Wave Function. Brazilian Journal of Developmen, v. 7, p. 20386-20399. doi: https://doi.org/10.34117/bjdv7n2-604

Sales, J. H. de O., & Girotto, P. H. S. (2021). Algoritmos para Equação Integral Quântico Não Relativístico. The Journal of Engineering and Exact Sciences, 7(3), 12699–01. doi: https://doi.org/10.18540/jcecvl7iss3pp12699-01-19e

Schmid, A. (1986). Quasiclassical wave function in multidimensional quantum decay problems. *Annals of Physics*, (170), 333-369. doi: https://doi.org/10.1016/0003-4916(86)90096-5

Takada, S., & Nakamura, H. (1994). Wentzel–Kramers–Brillouin theory of multidimensional tunneling: General theory for energy splitting. *The Journal of Chemical Physics*, (100), 98. doi: https://doi.org/10.1063/1.466899

Wang, X. W., & Lin, D. L. (1986). Multi-dimensional WKB treatment of first passage time. *Journal of Physics A: Mathematical and General*, (19), 1597. doi: https://doi.org/10.1088/0305-4470/19/9/032

Zamastil, J., Špirko, V., Čížek, J., Skála, L., & Bludský, O. (2001). Multidimensional WKB approximation and the lifetime calculation. *PHYSICAL REVIEW A*, (64), 042101. doi: https://doi.org/10.1103/PhysRevA.64.042101